[CANCER RESEARCH 62, 3555–3561, June 15, 2002]

Insulin Increases the Sensitivity of Tumors to Irradiation: Involvement of an Increase in Tumor Oxygenation Mediated by a Nitric Oxide-dependent Decrease of the Tumor Cells Oxygen Consumption[1]

Bénédicte F. Jordan, Vincent Grégoire, Roger J. Demeure, Pierre Sonveaux, Olivier Feron, Julia O'Hara, Valérie P. Vanhulle, Nathalie Delzenne, and Bernard Gallez[2]

Laboratory of Medicinal Chemistry and Radiopharmacy [B. F. J., B. G.], Laboratory of Biomedical Magnetic Resonance [B. F. J., R. J. D., B. G.], Radiobiology and Radioprotection Unit [V. G.], Laboratory of Pharmacotherapy [P. S., O. F.], and Laboratory of Pharmacokinetics, Metabolism, Nutrition and Toxicology [V. P. V., N. D.], Université Catholique de Louvain, B-1200 Brussels, Belgium, and EPR Research Center for the Study of Viable Biological Systems, Dartmouth Medical School, Hanover, New Hampshire 03755 [J. O.]

ABSTRACT

The effects of insulin on tumor oxygenation, perfusion, oxygen consumption, and radiation sensitivity were studied on two different mouse tumor models (TLT, a liver tumor, and FSAII, a fibrosarcoma). Anesthetized mice were infused with insulin i.v. at a rate of 16 milliUnits/kg/min for 25 min. Local tumor oxygenation measurements were carried out using two independent techniques: electron paramagnetic resonance oximetry and a fiber-optic device (OxyLite). Two complementary techniques were also used to assess the blood flow inside the tumor: a laser Doppler system (OxyFlo) and contrast-enhanced magnetic resonance imaging. The oxygen consumption rate of tumor cells after *in vivo* insulin infusion was measured using high frequency electron paramagnetic resonance oximetry. To know if insulin was able to enhance radiation-induced tumor regrowth delay, tumor-bearing mice were treated with 16 Gy of 250 kV radiation dose after insulin infusion.

We provide evidence that insulin increases the local pressure of oxygen of tumors (from 0–3 mm Hg to 8–11 mm Hg) as well as the tumor response to irradiation (increasing regrowth delay by a factor of 2.11). We found that the insulin-induced increase of tumor pressure of oxygen: (*a*) is not caused by an increase in the tumor blood flow, which is even decreased after insulin infusion; (*b*) is because of a decrease in the tumor cell oxygen consumption (*in vivo* insulin consumed oxygen three times slower than control cells); and (*c*) is inhibited by a nitric oxide (NO) synthase inhibitor, Nω-nitro-L-arginine methyl ester, when injected i.p. at 15 μmol/kg^{-1}, 1 h before insulin infusion. We demonstrate by immunoblotting that the NO pathway involves a phosphorylation of endothelial NO synthase and showed a concomitant increase in the cyclic GMP tumor level.

These findings provide unique insights into biological processes in tumors, new possible management for treating cancer patients, and raise major questions about the role of insulin secretion (fasting status and diabetes) in the clinical response of tumors to radiation therapy.

INTRODUCTION

Oxygen is a key environmental factor in the development and growth of tumors, and their response to treatment. Oxygen levels affect tumor cell metabolism, proliferation, and migration (1). Hypoxia can also stimulate angiogenesis (2). The partial pO_2[3] plays important roles in the response of tumors to cytotoxic treatments such as chemotherapy, radiotherapy, and photodynamic therapy. The recent technologies that now permit the assessment of flow and measurement of oxygen inside tissues push toward new strategies aimed at modulating flow and oxygenation in cancer treatment. These include a decrease of tumor oxygenation and blood flow in the antiangiogenic approach, and an increase of tumor oxygenation as a radiosensitizing approach. Up to now, in the sensitizing approach, most studies have used pharmacological interventions, modifying the oxygen supply with very encouraging experimental results. The use of vasoactive agents (3) or carbogen breathing, which is already used in Phase II clinical studies (4, 5), improved radiation response. Other interventions are aimed to radiosensitize hypoxic cells and have undergone promising Phase III clinical tests (6). However, only a few studies have focused on the role of the physiological conditions of the host tissues or on the role of hormones.

Initially, we made the assumption that insulin could be an important modulator of tumor oxygenation, because this hormone is known to change blood flow (oxygen supply; Refs. 7–9). In recent years, several studies have shown that hyperinsulinemia can increase blood flow in human skeletal muscle *in vivo* (10). They reported that i.v. insulin caused a dose-dependent increase in the rate of resting leg blood flow in humans, independent of hypoglycemia (11). A positron emission tomography study with ^{15}O water showed that hyperinsulinemia almost doubled skeletal muscle blood flow (12). Because the tumor models we used were implanted in the skeletal gastrocnemius muscle, we wanted to know if the tumor oxygenation could increase because of an increase in tumor blood flow, as it did in the muscle. Using two different tumor models, we demonstrate that insulin has a profound effect on tumor oxygenation. We actually found that the increase in tumor oxygenation was not because of an increase in tumor blood flow but because of a decrease in tumor cell oxygen consumption. We also demonstrated that the increase in tumor oxygenation was NO-dependent, because the effect was inhibited by the NOS inhibitor L-NAME. We also identified that the NO pathway involves a phosphorylation of eNOS and showed a concomitant increase in the cGMP tumor level. Finally, we found that insulin infusion increases the sensitivity of tumors to irradiation.

MATERIALS AND METHODS

Animal Tumor Models

Two different tumor models were implanted in the thigh of mice: a transplantable liver tumor model (TLT; Ref. 13) on NMRI mice and the syngeneic FSAII tumor model (14) on C3H mice. A total of 126 animals were used for this study.

Treatment

Anesthesia was first induced by an i.p. injection of ketamine (80 mg/kg)/xylazine (8 mg/kg) and maintained with ketamine alone (30 mg/kg). Insulin (Actrapid HM; Novo Nordisk, Bagsvaerd, Denmark) was infused i.v. at a rate

Received 11/13/01; accepted 4/18/02.

The costs of publication of this article were defrayed in part by the payment of page charges. This article must therefore be hereby marked *advertisement* in accordance with 18 U.S.C. Section 1734 solely to indicate this fact.

[1] Supported by the Belgian National Fund for Scientific Research (FRSM 3.4560.00) and the Fonds Joseph Maisin. B. F. J. and P. S. are Research Assistants of the Belgian National Fund for Scientific Research. O. F. is Research Associate of the Belgian National Fund for Scientific Research.

[2] To whom requests for reprints should be addressed, at Laboratory of Medicinal Chemistry and Radiopharmacy, Avenue Mounier 73.40, B-1200 Brussels, Belgium. E-mail: Gallez@cmfa.ucl.ac.be.

[3] The abbreviations used are: pO_2, pressure of oxygen; EPR, electron paramagnetic resonance; MRI, magnetic resonance imaging; cGMP, cyclic GMP; NOS, nitric oxide synthase; L-NAME, *N*-nitro-L-arginine methyl ester; eNOS, endothelial nitric oxide synthase; NO, nitric oxide; DTPA, diethylenetriaminepentaacetic acid; P-eNOS, phosphorylated endothelial nitric oxide synthase; RX, radiation dose.

of 16 mU/kg/min for 25 min. The dose of insulin was chosen as one known to modify the skeletal muscle blood flow on rodents. Carbogen (5% CO_2/95% O_2) breathing (5 liter/min) was used as a reference treatment. The control group was infused with a 0.9% NaCl solution only. When used, the NOS inhibitor, Nω-nitro-L-arginine methyl ester (Sigma, Steinheim, Germany) was injected i.p. at 15 μmol/kg^{-1}, 1 h before insulin infusion (15).

pO_2 and Blood Flow Measurements

Local tumor oxygenation measurements were carried out using two independent techniques: EPR oximetry and a fiber-optic device, OxyLite. We also used two complementary techniques to assess the blood flow inside the tumor: the OxyFlo system and contrast-enhanced MRI. Mice were maintained at 37°C using an homeothermic blanket.

EPR Oximetry. EPR spectra were recorded using an EPR spectrometer (Magnettech, Berlin, Germany) with a low frequency microwave bridge operating at 1.1 GHz and extended loop resonator. Charcoal (Charcoal wood powder, CX0670–1; EM Science, Gibbstown, NJ) was used as the oxygen-sensitive probe in all of the experiments. Calibrations curves were made by measuring the EPR line width as a function of the pO_2. For this purpose, the charcoal was suspended in a tumor homogenate, and EPR spectra were obtained on a Bruker EMX EPR spectrometer (9 GHz) between 0 and 21% O_2. Nitrogen and air were mixed in an Aalborg gas mixer (Monsey, NY), and the oxygen content was analyzed using a servomex oxygen analyzer OA540 (16). Mice were injected in the center of the tumor (8-mm diameter) using the suspension of charcoal (100 mg/ml, 50-μl injected, 1–25-μm particle size). The EPR measurements were started 2 days after the injection. The tumor under study was placed in the center of the extended loop resonator, which sensitive volume extended 1 cm into the tumor mass, using a protocol described previously (3, 17). The localized EPR measurements correspond to an average of pO_2 values in a volume of $\sim$10 mm^3 (3).

OxyLite/OxyFlo Technique. We used the OxyLite in conjunction with OxyFlo (Oxford Optronix, Oxford, United Kingdom) for simultaneously and continuously monitoring tissue blood flow, oxygenation, and temperature at the same location (18, 19). Fiber-optic microprobes combining a laser Doppler system, an oxygen-sensor, and a thermocouple were inserted both into the tumor and in the muscle. Data were collected continuously at a sampling frequency of 20 Hz, before, during, and 35 min after insulin infusion. OxyLite pO_2 measurements are single point measurements, and the volume sampled is confined to the sensor tip (230-μm diameter). Braun *et al.* (20) estimated that the probe would measure an average pO_2 in an area of $\sim$40,000 μm^2.

MR Experiments. MRI acquisitions were performed with a 4.7 Tesla Bruker Biospec experimental imager. Mice were maintained at 37°C during the experiments by flushing warm air inside the magnet. A preliminary anatomical rapid T_2 image [Rapid Acquisition with Relaxation Enhancement (RARE) sequence: time of repetition (TR) = 1500 ms, time of echo (TE) = 11.5 ms, 4 averages, echo train length = 8] was acquired to define a region of interest encompassing the whole tumor. Dynamic Gd-DTPA (FLASH imaging) before and after i.v. administration of insulin were performed: TR = 5 ms, TE = 5 ms, $\propto$; = 5°, matrix size = 64*64, field of view = 6 cm. A Gd-DTPA uptake experiment consisted of 40 consecutive T1-weighted FLASH images with a total acquisition time of 40 s. Gd-DTPA in 0.9% NaCl solution was injected as an i.v. bolus injection (180 μl, 1 s duration, 0.2 mmol/kg) after five precontrast images. Each mouse received a first bolus of Gd-DTPA alone (constituting the control part of the experiment). Signal intensity had decreased to the basal level after 2 h, so the second bolus injection was performed 2 h after the first one. For the treated group, the insulin infusion (25 min) was completed 30 min before the second contrast agent injection. The two uptake curves were then compared (5).

Oxygen Consumption Rate Evaluation

The method developed by James *et al.* (21) was used. All of the spectra were recorded on a Bruker EMX EPR spectrometer operating at 9 GHz. Mice were first treated with insulin *in vivo*. Thirty min after the end of insulin infusion, tumors were excised, trypsinized for 30 min, and cell viability determined as reported previously (21). Cells (2×10^7/ml) were suspended in 10% dextran in complete medium. A neutral nitroxide, ^{15}N 4-oxo-2,2,6,6-tetramethylpiperidine-d$_{16}$-^{15}N-1-oxyl at 0.2 mM (CDN Isotopes, Pointe-Claire, Quebec, Canada), was added to 100-μl aliquots of tumor cells that were then drawn into glass capillary tubes. The probe (0.2 mM in 20% dextran in complete medium) was calibrated at various O_2 between 100% nitrogen and air so that the line width measurements could be related to O_2 at any value. Nitrogen and air were mixed in an Aalborg gas mixer, and the oxygen content was analyzed using a servomex oxygen analyzer OA540. The sealed tubes were placed into quartz ESR tubes, and samples were maintained at 37°C. As the resulting line width reports on O_2, oxygen consumption rates were obtained by measuring the O_2 in the closed tube over time and finding the slope of the resulting linear plot.

Irradiation and Tumor Regrowth Delay Assay

The tumor-bearing leg was locally irradiated with 16 Gy of 250 kV X-rays (RT 250; Philips Medical Systems). Mice were anesthetized, and the tumor was centered in a 3-cm diameter circular irradiation field. When tumors reached 8.0 $\pm$ 0.5 mm in diameter, the mice were randomly assigned to a treatment group and irradiated. After treatment, tumors were measured every day until they reached a diameter of 16 mm, at which time the mice were sacrificed. A linear fit could be obtained between 8 and 16 mm, which allowed us to determine the time to reach a particular size for each mouse. For each tumor, transversal and antero-posterior measurements were obtained. An average tumor diameter was then calculated.

Metabolic Parameters Quantification

The measurements were performed on FSAII tumors and on leg muscles (before treatment and 30 min after insulin infusion).

ATP Content. Tumor and muscles slices were taken, washed twice in NaCl solution. and sonicated in 1 ml of 2% perchloric acid. The intracellular ATP content was measured on neutralized perchloric acid extracts using ATP Bioluminescence Assay kit CLS II from Boehringer (Brussels, Belgium).

Lactate Content. Tumor slices were taken, washed twice in NaCl solution, and sonicated in 2 ml of 3.65% perchloric acid. This deproteinization was performed twice. The lactate content was measured on neutralized extracts using the Lactate kit from Sigma Diagnostics (Bornem, Belgium).

Glycogen Content. Tumor and muscle slices were taken, rapidly washed twice in NaCl solution, sonicated in 1 ml of 1 M KOH, then heated at 100°C for 10 min. After neutralization with acetic acid and centrifugation, the supernatant was incubated in the presence of α-amylo glucosidase in pH 5 acetate buffer (1 M). The glucose produced was quantified by an enzymatic reaction as described elsewhere (22).

Blood Glucose Level. Blood samples were taken and centrifuged at 4°C. The analysis was performed on serum using the Glucose kit from Elitech Diagnostics (Sees, France).

Identification of the NO Pathway

Immunoblotting. Insulin-treated or control FSAII-bearing mice were sacrificed, and tumors were homogenized in a buffer containing phosphatase and protease inhibitors (23). Samples were equally loaded and processed for immunoblotting as described elsewhere (24). P-eNOS antibody was from NEB Cell Signaling Technology (Beverly, MA), eNOS antibody from BD Transduction Labs (Lexington, KY).

cGMP Quantification. Insulin-treated or control FSAII-bearing mice were sacrificed, and tumors were homogenized in cold 6% (w/v) trichloroacetic acid. Samples were then centrifuged at 2000 $\times$ *g* for 15 min at 4°C. The supernatant was washed four times with 5 volumes of water-saturated diethyl ether. The aqueous extract remaining was dried under a stream of nitrogen at 60°C, and the dried extract was dissolved in a 0.05 M sodium acetate buffer pH 5.8 containing 0.02% (w/v) BSA before analysis. The cGMP content was then determined by the cGMP enzyme immunoassay kit from Biotrak (Amersham Pharmacia Biotech Europe GmbH, Freiburg, Germany).

Statistical Analysis

Results are presented as means $\pm$ SE. Comparisons between groups were analyzed by *t* test (two-sided) or ANOVA for experiments with more than two subgroups. In this case, the Dunnet PostHoc test was considered. *P*s < 0.05 were considered statistically significant.

RESULTS

Effect of Insulin Infusion on the Tumor Oxygenation. EPR oximetry relies on the oxygen-dependent broadening of the EPR line width of a paramagnetic oxygen sensor implanted in the tumor (3, 25). The fiber-optic device, OxyLite, allows pO_2 measurement that is based on the oxygen-quenched lifetime of a luminescent ruthenium dye (18, 19). The two techniques we used are intended for continuous measurement of the local pO_2 without altering the local oxygen concentration, and allow a real-time study of the oxygen fluctuations in tissues. Insulin infusion modified tumor pO_2 for both models. Oxygenation slowly increased during insulin infusion and continued to increase after the end of the infusion (Fig. 1; Table 1). Prolonged experiments carried out on 4 mice indicate that the tumor pO_2 reached its maximum value within 25–30 min after the end of the infusion and fell to the basal value within 6–7 h (data not shown). Carbogen breathing, used as a positive control, induced an increase of 23.2 mm Hg and 18.7 mm Hg for TLT and FSAII tumor models, respectively ($n = 10$). A typical experiment is shown on Fig. 1. All of the results are summarized in Table 1.

Effect of Insulin Infusion on the Tumor Blood Flow. We used two complementary techniques to assess the blood flow inside the tumor: the OxyFlo system based on laser-Doppler flowmetry, and contrast-enhanced MRI that compares the vascular distribution of a paramagnetic contrast agent, Gd-DTPA, before and after insulin infusion. Using OxyFlo, we found that the flow remained unchanged (2 of 5 tumors) or was decreased (3 of 5) during and after insulin infusion. On both tumor models, the MRI analysis confirmed the decrease of the flow because the signal enhancement on Gd-DTPA contrast-enhanced images was lower for the insulin-treated group than for the control group (Fig. 2; $n = 4$/group; $P = 0.021$). Because the "control" and "insulin curves" were performed on the same mouse, we avoided external perturbations from different tumor size, vascularization, or contrast agent clearance. A pixel by pixel analysis demonstrated that 32–60% of the pixels contributed to the blood flow decrease of the tumor after insulin infusion. The increase in blood flow in the muscle did not lead to an increase in flow inside the tumor in this case: the increase in normal tissue blood flow because of vasodilation (29.2 ± 6.8% increase in the flow in the muscle after insulin infusion; $n = 5$; data not shown) shunted away the blood flow from the tumor to the muscle ("steal effect"). Therefore, the increase in pO_2 cannot be assigned to an increase of the oxygen supply.

Effect of Insulin Infusion on the Oxygen Consumption Rate by Tumor Cells. We measured the oxygen consumption rate of tumor cells extracted from the tumors of mice infused with a 0.9% NaCl solution or with insulin. *In vivo* tumor pretreatment with insulin reduced the rate of oxygen consumption by the tumor cells (Fig. 3). The mean slopes were −0.80 μM/min ± 0.02 and −0.26 ± 0.06 μM/min for control and insulin groups, respectively ($n = 4$ for each group). This means that *in vivo* insulin pretreated cells consumed oxygen three times slower than control cells. We concluded that the tumor oxygenation increase was because of the decrease of the oxygen consumption by the tumor cells.

Bioenergetic Parameters Modified by Insulin Infusion. A variety of biological mechanisms, involving the interaction between tumor cells and their metabolic microenvironment (oxygen supply and the bioenergetic status), is involved in the lack of responsiveness of solid tumors to nonsurgical treatments. To identify the origin of the change in tumor oxygenation and oxygen consumption by tumor cells, some bioenergetic parameters of the tumor were quantified before and after insulin treatment. Blood glucose levels decreased from 13.4 ± 2.5 mM for the control group to 7.9 ± 2.4 mM for the insulin treated group ($n = 9$; $P = 0.013$). The ATP tumor concentration rose from 5.1 nmol/mg protein to 16.4 nmol/mg protein 30 min after the end of the infusion ($n = 9$; $P = 0.012$), whereas no significant modifications were observed in muscle. The lactate tumor content rose from 358 ± 38 mg/mg protein to 545 ± 55 mg/mg protein ($n = 12$; $P = 0.027$). No change was observed in tumor and muscle glycogen content after insulin infusion ($n = 9$; $P > 0.05$). These results suggest that the increase in ATP content in tumor cells is because of the orientation of glucose toward the anaerobic glycolytic pathway, because oxygen consumption is decreased with insulin, or is because of the sparing of the newly synthesized ATP, which is not used for glycogen synthesis in tumor cells. The observed increase in the tumor lactate content is an indicator of an increase of the anaerobic glycolytic pathway activity. The factors underlying anaerobic glycolysis in tumor cells are now well documented (26).

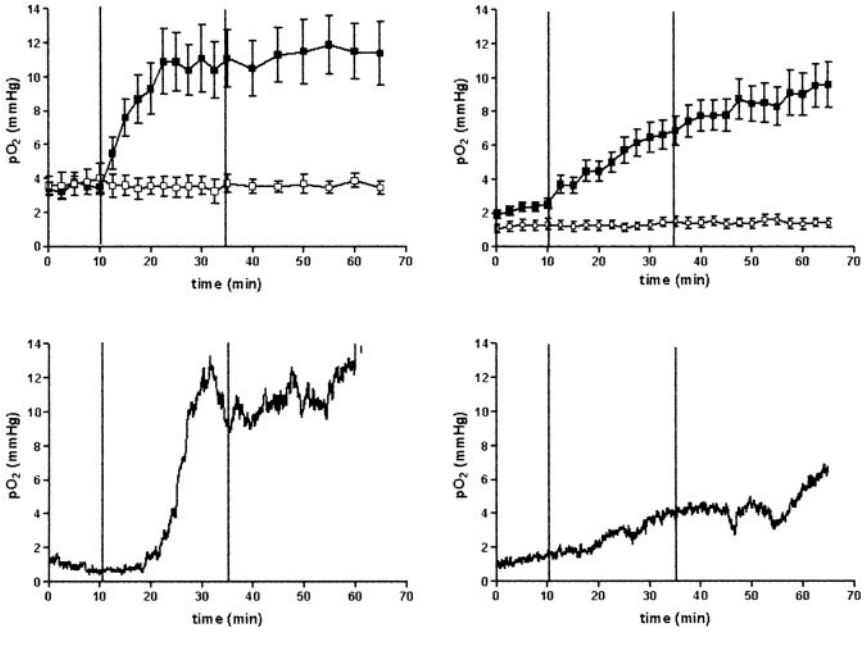

Fig. 1. Effect of insulin infusion on tumor pO_2. *Top*, tumor pO_2 monitored by EPR oximetry [before (0–10 min)/during (10–35 min)/and after insulin infusion (35–65 min)]. □, control group; ■, insulin-treated group. *Left*, FSA II ($n = 5$/group); *right*, TLT ($n = 10$/group). *Bottom*, typical tumor pO_2 monitored by OxyLite oximetry (before/during/and after insulin infusion). *Left*, FSA II; *right*, TLT. Note the significant increase in tumor pO_2 for both tumor models; *bars*, ±SE.

Table 1 *Effect of the treatment on the tumor pO_2*

Local tumor oxygenation measurements were carried out using two independent techniques: EPR oximetry and a fibre-optic device (OxyLite). Insulin was infused intravenously at a rate of 16 mU/kg/min for 25 minutes. Carbogen breathing (5 liter/min) was used as a reference treatment. The control group was infused with a 0.9% NaCl solution only.

		EPR		Oxylite	
Tumor model	Treatment	Pre (mm Hg)	post (30 min) (mm Hg)	Pre (mm Hg)	post (30 min) (mm Hg)
TLT	insulin	1.9 ± 0.2	9.6 ± 1.4[a]	1.6 ± 0.5	8.4 ± 2.2[a]
	carbogen	1.0 ± 0.3	24.2 ± 5.1[a]	0.9 ± 0.5	13.2 ± 5.1[a]
	control	1.1 ± 0.3	1.4 ± 0.3	1.9 ± 0.4	1.6 ± 0.5
FSAII	insulin	3.4 ± 0.4	11.4 ± 1.9[a]	2.3 ± 0.3	10.3 ± 2.2[a]
	carbogen	2.7 ± 0.5	21.4 ± 3.7[a]	2.0 ± 0.7	21.0 ± 8.5[a]
	control	3.6 ± 0.6	3.5 ± 0.4	1.8 ± 0.7	1.9 ± 0.7

[a] $P<0.05$.

Insulin Increases the Tumor Oxygenation by a NO-dependent Pathway. We made the hypothesis that the decrease in tumor cell oxygen consumption could be mediated by a NO pathway, because insulin exerts cardiovascular actions that are mediated at least in part by this system. To verify the involvement of NO in the effect of insulin on tumor oxygenation, a group of FSAII tumors was treated with L-NAME 1 h before insulin infusion. We observed that this NOS inhibitor abolished the effect of insulin on tumor pO_2 (Fig. 4). In addition, we identified by immunoblotting that eNOS was the only detectable NOS isoform in FSAII tumors (not shown) and importantly, was activated by phosphorylation after *in vivo* insulin infusion. P-eNOS was present in samples obtained from insulin-treated tumors and absent in control ones ($n = 3$/group; Fig. 5), whereas there was no significant difference in eNOS abundance between insulin and control groups ($P > 0.05$). Finally, we showed that the cGMP level of the tumor significantly increased after insulin infusion ($P = 0.013$) compared with control tumors (Fig. 6).

Effect of Insulin Infusion on the Sensitivity of Tumors to Irradiation. To determine whether insulin had an effect on the tumor response to radiotherapy, FSAII tumor-bearing mice were treated with irradiation alone, with the combination of insulin and irradiation, or with the combination of L-NAME 1 h before insulin infusion followed by irradiation, and the tumor regrowth delays were measured. A preliminary study indicated that insulin alone had no effect on tumor growth. Because the FSA II tumor model is known to be radiosensitized by carbogen (27), we compared the effect of carbogen breathing during irradiation to the effects of insulin infusion. To avoid tumor cure but still achieve a measurable regrowth delay, a single irradiation dose of 16 Gy was selected as the RX after preliminary tests. The regrowth delay to reach 12-mm tumor diameter was 4.6 ± 0.3 days for RX alone, 7.4 ± 0.3 days for carbogen and RX ($P = 3.8*10^{-5}$), and 9.7 ± 0.2 days for insulin and RX ($P = 4.9*10^{-7}$; Fig. 7). These data indicate that insulin increased the sensitivity of the tumor to X-ray irradiation, increasing regrowth delay by a factor of 2.11 compared with a factor of 1.61 for carbogen, treatment that is currently being used successfully in the clinic (4). The L-NAME pretreated group, additionally infused with insulin and irradiated, is similar to the RX group ($P > 0.05$), with a regrowth delay of 5.1 ± 0.7 days (Fig. 7). L-NAME administration before insulin infusion totally inhibited the radiosensitizing effect of insulin. L-NAME administration before irradiation (without insulin treatment) had no effect on the tumor regrowth delay on this tumor model (the "RX" and "L-NAME + RX" curves are similar; Fig. 7).

DISCUSSION

For the first time, we report that insulin can modulate tumor perfusion and oxygenation. The decrease in perfusion is likely to be because of a vascular steal effect with a redistribution of the blood flow that feeds the tumor and the muscle. The increase in tumor oxygenation is related to the decrease in oxygen consumption by the tumor cells. It has indeed been predicted theoretically that modification of oxygen consumption is much more efficient at affecting oxygen transport than modification of delivery (28). Our experiments

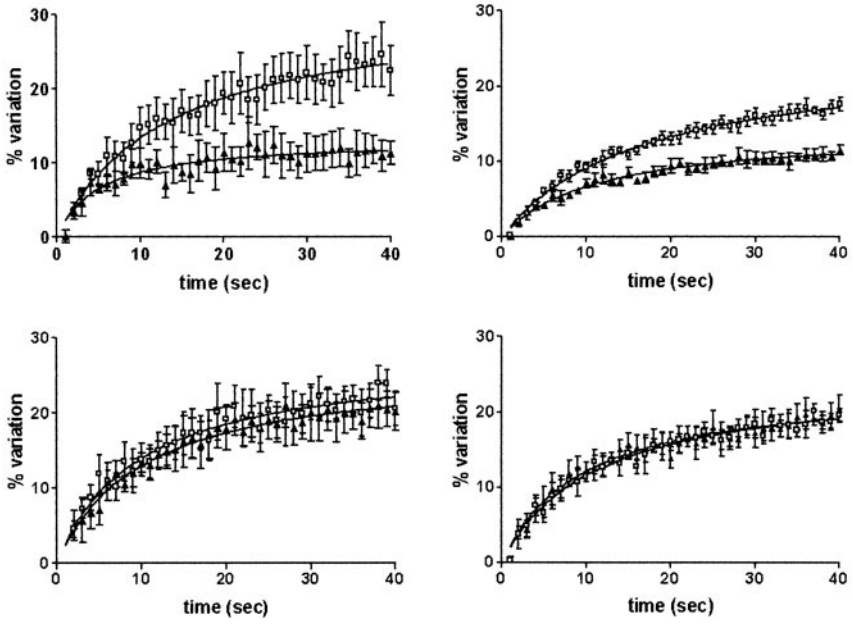

Fig. 2. Effect of insulin infusion on the tumor blood flow. Dynamic Gd-DTPA FLASH imaging for FSAII (*left*) and TLT (*right*) tumors. *Top*, insulin-treated mice. *Bottom*, control experiment. □, % variation of signal intensity after the first Gd-DTPA bolus injection; ▲, % of MRI signal enhancement after the second Gd-DTPA bolus injection ($n = 4$/group). Note the significant decrease in signal enhancement after the second Gd-DTPA injection for the insulin-treated group, whereas both curves are superimposable for the control group; *bars*, ± SE.

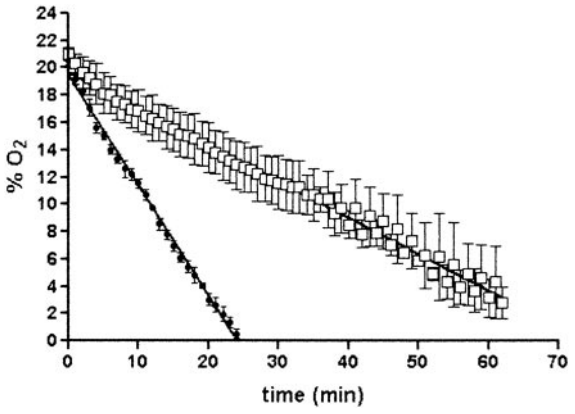

Fig. 3. Effect of insulin infusion on tumor cell oxygen consumption rate. FSA II tumor cells oxygen consumption rate (n = 4/group). □, insulin-treated group; ●, control group. Mean slopes: −0.80 μM/min ±0.02 and −0.26 ± 0.06 μM/min for control and insulin groups, respectively (n = 4 for each group). *In vivo* insulin-pretreated cells consumed oxygen three times slower than control cells; *bars*, ±SE.

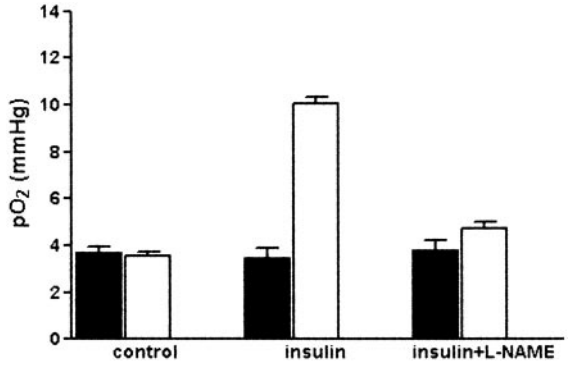

Fig. 4. Effect of L-NAME administration 1 h before insulin treatment on FSAII tumor pO_2. ■, basal pO_2 (before insulin treatment), □, final pO_2 (30 min after the end of insulin infusion). Each *bar* represents the mean pO_2 value ± SE of 5 tumors.

demonstrate that the likely scenario involves a stimulation of NOS, because a phosphorylation of eNOS was shown (without exclusion of other possible pathways). It was shown previously that NO affects the oxygen consumption of skeletal muscles. Basal NO release inhibits oxygen consumption in muscle (29). NO donors decrease oxygen consumption, an effect that is blocked by L-NAME (30). NOS inhibitors have also been shown to increase oxygen consumption in healthy human volunteers (31). Much evidence has since proven that NO regulates mitochondrial respiration by virtue of reversible interactions with cytochrome *c* oxidase (complex IV in the mitochondrial respiratory chain). In brief, cytochrome *c* oxidase, modulated by the NO:oxygen ratio, acted as an oxygen sensor. Low concentrations of NO, continuously generated by NOS, explained the decrease in respiration that occurred at low oxygen concentration (32). In this case, insulin did stimulate eNOS and could, thus, increase NO release, and decrease cell respiration and oxygen (the basal pO_2 of the tumor being very low). This decrease in oxygen consumption could, hence, induce a progressive increase in tumor pO_2 as observed in our studies.

Corroborating this mechanism, it has been found that $eNOS^{-/-}$ mice were hypertensive but also insulin-resistant, as evidenced by fasting hyperinsulinemia and a 40% lower insulin-stimulated glucose uptake. Insulin resistance in $eNOS^{-/-}$ mice was related specifically to impaired NO synthesis, because in hypertensive mice induced by a model of renovascular hypertension, insulin-stimulated glucose uptake was normal (vascular NO production was evaluated by measurement of plasma concentration of nitrite and nitrate; Ref. 33).

Because ketamine has well-described effects on mobilization of glucose reserves and blood glucose levels (34), the effect of insulin infusion on the tumor pO_2 was also tested on mice anesthetized with isoflurane. It was similar to that of ketamine/xylazine anesthetized mice (data not shown).

The action of insulin on vascular endothelium is thought to couple regulation of hemodynamic homeostasis with metabolic homeostasis. Physiologically, most of these vascular effects appear mediated by NO. Our current findings additionally emphasize the critical role of this insulin/NO pathway in tumors. NO has the unique ability to either initiate or arrest tumor formation: this multifaceted role clearly depends on a variety of conditions that exist in the tumor environment. Here, we demonstrate that when acutely controlling its production, *e.g.*, by insulin administration, the properties of NO can be exploited to potentiate the tumoricidal effects of irradiation.

One straightforward application of the present study is to take advantage of the radiosensitizing effect of the slow infusion of insulin. Because insulin clamp (slow insulin infusion) is already used in specific clinical applications for estimation of insulin sensitivity (35, 36), the use of such a protocol can be immediately tested in patients. We showed that insulin radiosensitized FSAII tumors *in vivo*, with a regrowth delay even higher than using the carbogen treatment. We can speculate why insulin is more efficient in radiosensitizing FSAII tumors than carbogen when carbogen induces a greater increase in tumor pO_2. Besides the radiosensitizing effect attributable to oxygen, insulin has been shown to inhibit repair of potentially lethal radiation damage. Johnson *et al.* (37) showed that the average completion time of an excision repair patch varied according to the state of cell culture and that the completion time was extended after treatment with insulin. Subsequently insulin has been shown to inhibit repair of radiation damage and chromosome aberrations (38). Finally, an additional effect of NO itself cannot be excluded, because NO has been

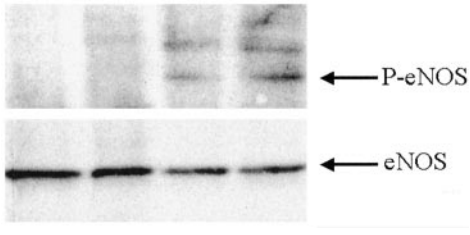

Fig. 5. eNOS phosphorylation after insulin treatment of FSAII tumor-bearing mice detected by immunoblotting (144 kDa). Mice were untreated (*left*) or infused with insulin before tumor excision (*right*). *Top*, P-eNOS; *bottom*, e-NOS. Note the presence of P-eNOS for the insulin-pretreated mice.

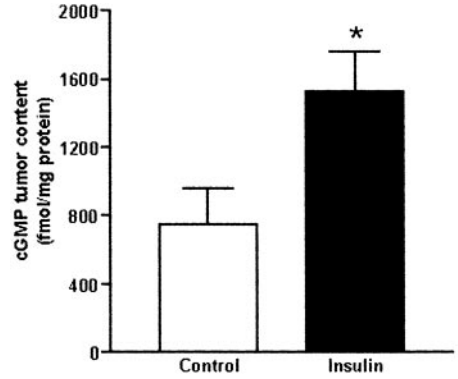

Fig. 6. Effect of insulin infusion on the cGMP tumor content. Each *bar* represents the mean value (fmol/mg protein) ± SE. □, control group (n = 3); ■, insulin group (n = 3).

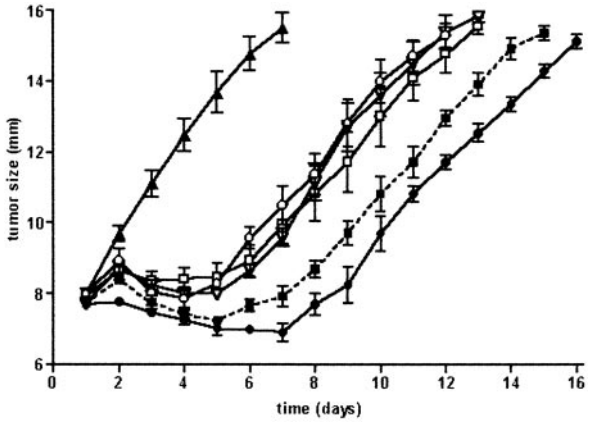

Fig. 7. Effect of the combination of insulin and radiation on FSAII tumor regrowth. Mice were untreated (▲), treated with 16 Gy of RX alone (○), infused with insulin before 16 Gy of RX (●), treated with carbogen 15 min before and during irradiation with 16 Gy of RX (—■—), pretreated with L-NAME one h before insulin infusion and irradiated with 16 Gy of RX (□), or treated with L-NAME alone and irradiated with 16 Gy of RX (▽) Each *point* represents the mean tumor size ± SE of 6 tumors. The regrowth delay to reach 12-mm tumor diameter was 4.8 ± 0.6 days for RX alone, and 9.1 ± 1.1 days for insulin and RX ($P = 0.008$). Insulin increased the regrowth delay by a factor of 1.9.

shown to be a radiosensitizer of hypoxic cells *in vitro* (39) and *in vivo* (40).

Drugs that inhibit respiration, such as meta-iodobenzylguanidine were proposed as potential radiosensitizing agents (41). Mild hyperglycemia, which has also been demonstrated to reduce oxygen consumption (Crabtree effect), has been tested recently in combination with hyperoxic gas (42). It is reasonable to assume that the increase in pO_2 observed after hyperglycemia can at least partly be explained by a stimulation of insulin secretion and a consequent reduction of oxygen consumption. Because insulin acts by decreasing the oxygen consumption of tumor cells, this approach could be complementary to strategies modifying the oxygen supply in the tumor (*i.e.*, carbogen breathing). However, insulin infusion is not indicated as a sensitizing approach for chemotherapy as the perfusion of the tumor was decreased after that treatment.

Besides the effect of acute injection of insulin on the circulation and the oxygenation of the tumor, our study might have implications for additional studies on the role of the physiology of the host on the tumor response to treatments. What could be the role of inadequate secretion of insulin in a chronic situation? Chronic diabetes often is suggested as a complicating factor for damage in normal tissues in the radiation field and even recently claimed as a predictor for late radiation morbidity (43). Although many factors can be evoked in diabetes mellitus such as alterations in blood viscosity and microvascular occlusive changes, our study isolates one factor with major implications in the tumor biology that should be additionally investigated.

Our results indicate that an important consideration may be the influence of the fasting status of patients before irradiation. Because insulin secretion is dependent on feeding, it is likely that the tumor blood flow and oxygenation will be modified after a meal. Up to now, the influence of fasting was studied only in very few early works on a possible radioprotective effect on whole-body irradiated mice (44, 45). The biodistribution of therapeutic or diagnostic radionuclides has been found to be dependent on food ingestion (46). Again, it is likely that the fasting status and consequent insulin blood concentration should carefully be taken into account in monitoring treatments in animal models as well as in the clinical situation.

ACKNOWLEDGMENTS

We thank Jean-Luc Balligand and Stanislas Pauwels for helpful discussions.

REFERENCES

1. Vaupel, P., Kallinowski, F., and Okunieff, P. Blood flow, oxygen and nutrient supply, and metabolic microenvironment of human tumors: a review. Cancer. Res., *49:* 6449–6465, 1989.
2. Shweiki, D., Itin, A., Soffer, D., and Keshet, E. Vascular endothelial growth factor induced by hypoxia may mediate hypoxia-initiated angiogenesis. Nature (Lond.), *359:* 843–845, 1992.
3. Gallez, B., Jordan, B. F., Baudelet, C., and Misson, P. D. Pharmacological modifications of the partial pressure of oxygen in murine tumors: evaluation using *in vivo* EPR oximetry. Magn. Reson. Med., *42:* 627–630, 1999.
4. Wijffels, K. I., Kaanders, J. H., Rijken, P. F., Bussink, J., van den Hoogen, F. J., Marres, H. A., de Wilde, P. C., Raleigh, J. A., and van der Kogel, A. J. Vascular architecture and hypoxic profiles in human head and neck squamous cell carcinomas. Br. J. Cancer, *83:* 674–683, 2000.
5. van der Sanden, B. P., Heerschap, A., Hoofd, L., Simonetti, A. W., Nicolay, K., van der Toorn, A., Colier, W. N., and van der Kogel, A. J. Effect of carbogen breathing on the physiological profile of human glioma xenografts. Magn. Reson. Med., *42:* 490–499, 1999.
6. Brown, J. M. The hypoxic cell: a target for selective cancer therapy–eighteenth Bruce F. Cain Memorial Award Lecture. Cancer Res., *59:* 5863–5870, 1999.
7. Steinberg, H. O., Brechtel, G., Johnson, A., Fineberg, N., and Baron, A. D. Insulin-mediated skeletal muscle vasodilation is nitric oxide dependent. A novel action of insulin to increase nitric oxide release. J. Clin. Investig., *94:* 1172–1179, 1994.
8. Sartori, C., Trueb, L., Nicod, P., and Scherrer, U. Effects of sympathectomy and nitric oxide synthase inhibition on vascular actions of insulin in humans. Hypertension (Dallas), *34:* 586–589, 1999.
9. Trovati, M., Massucco, P., Mattiello, L., Cavalot, F., Mularoni, E., Hahn, A., and Anfossi, G. Insulin increases cyclic nucleotide content in human vascular smooth muscle cells: a mechanism potentially involved in insulin-induced modulation of vascular tone. Diabetologia, *38:* 936–941, 1995.
10. Baron, A. D. Hemodynamic actions of insulin. Am. J. Physiol., *267:* E187–E202, 1994.
11. Laakso, M., Edelman, S. V., Brechtel, G., and Baron, A. D. Decreased effect of insulin to stimulate skeletal muscle blood flow in obese man. A novel mechanism for insulin resistance. J. Clin. Investig., *85:* 1844–1852, 1990.
12. Vicini, P., Bonadonna, R. C., Utriainen, T., Nuutila, P., Raitakari, M., Yki-Jarvinen, H., and Cobelli, C. Estimation of blood flow heterogeneity distribution in human skeletal muscle from positron emission tomography data. Ann. Biomed. Eng., *25:* 906–910, 1997.
13. Taper, H., Woolley, G. W., Teller, M. N., and Lardis, M. P. A new transplantable mouse liver tumor of spontaneous origin. Cancer Res., *26*: 143–148, 1966.
14. Volpe, J. P., Hunter, N., Basic, I., and Milas, L. Metastatic properties of murine sarcomas and carcinomas I. Positive correlation with lung colonization and lack of correlation with s. c. tumor take. Clin. Exp. Metastasis, *3:* 281–294, 1985.
15. Conner, E. M. Duration of the hemodynamic effects of N(G)-nitro-L-arginine methyl ester *in vivo*. Nitric Oxide, *4:* 85–93, 2000.
16. Jordan, B. F., Baudelet, C., and Gallez, B. Carbon-centered radicals as oxygen sensors for *in vivo* electron paramagnetic resonance: screening for an optimal probe among commercially available charcoals. Magn. Reson. Mater. Phys. Med. Biol. *7:* 121–129, 1998.
17. Jordan, B. F., Misson, P., Demeure, R., Baudelet, C., Beghein, N., and Gallez, B. Changes in tumor oxygenation/perfusion induced by the NO donor, isosorbide dinitrate, in comparison with carbogen: monitoring by EPR and MRI. Int. J. Radiat. Oncol. Biol. Phys., *48:* 565–570, 2000.
18. Collingridge, D. R., Young, W. K., Vojnovic, B., Wardman, P., Lynch, E. M., Hill, S. A., and Chaplin, D. J. Measurement of tumor oxygenation: a comparison between polarographic needle electrodes and a time-resolved luminescence-based optical sensor. Radiat. Res. *147:* 329–334, 1997.
19. Griffiths, J. R., and Robinson, S. P. The OxyLite: a fibre-optic oxygen sensor. Br. J. Radiol., *72:* 627–630, 1999.
20. Braun, R. D., Lanzen, J. L., Snyder, S. A., and Dewhirst, M. W. Comparison of tumor and normal tissue oxygen tension measurements using OxyLite or microelectrodes in rodents. Am. J. Physiol., *280:* H2533–H2544, 2001.
21. James, P. E., Jackson, S. K., Grinberg, O. Y., and Swartz, H. M. The effects of endotoxin on oxygen consumption of various cell types *in vitro:* an EPR oximetry study. Free Radic. Biol. Med., *18:* 641–647, 1995.
22. Krack, G., Goethals, F., Deboyser, D., and Roberfroid, M. Interference of chemicals with glycogen metabolism in isolated hepatocytes. Toxicology, *18:* 213–223, 1980.
23. Garcia-Cardena, G., Fan, R., Shah, V., Sorrentino, R., Cirino, G., Papapetropoulos, A., and Sessa, W. C. Dynamic activation of endothelial nitric oxide synthase by Hsp90. Nature (Lond.), *392:* 821–824, 1998.
24. Feron, O., Saldana, F., Michel, J. B., and Michel, T. The endothelial nitric-oxide synthase-caveolin regulatory cycle. J. Biol. Chem., *273:* 3125–3128, 1998.
25. Swartz, H. M., and Clarkson, R. B. The measurement of oxygen *in vivo* using EPR techniques, Phys. Med. Biol., *43:* 1957–1975, 1998.
26. Waki, A., Fujibayashi, Y., Yonekura, Y., Sadato, N., Ishii, Y., and Yokoyama, A. Reassessment of FDG uptake in tumor cells: high FDG uptake as a reflection of oxygen-independent glycolysis dominant energy production. Nucl. Med. Biol., *24:* 665–670, 1997.

27. Griffin, R. J., Okajima, K., and Song, C. W. The optimal combination of hyperthermia and carbogen breathing to increase tumor oxygenation and radiation response. Int. J. Radiat. Oncol. Biol. Phys., *42:* 865–869, 1998.
28. Secomb, T. W., Hsu, R., Ong, E. T., Gross, J. F., and Dewhirst, M. W. Analysis of the effects of oxygen supply and demand on hypoxic fraction in tumors. Acta Oncol., *34:* 313–316, 1995.
29. King, C. E., Melinyshyn, M. J., Mewburn, J. D., Curtis, S. E., Winn, M. J., Cain, S. M., and Chapler, C. K. Canine hindlimb blood flow and O_2 uptake after inhibition of EDRF/NO synthesis. J. Appl. Physiol., *76:* 1166–1171, 1994.
30. Shen, W., Xu, X., Ochoa, M., Zhao, G., Wolin, M. S., and Hintze, T. H. Role of nitric oxide in the regulation of oxygen consumption in conscious dogs. Circ. Res., *75:* 1086–1095, 1994.
31. Gilligan, D. M., Panza, J. A., Kilcoyne, C. M., Waclawiw, M. A., Casino, P. R., and Quyyumi, A. A. Contribution of endothelium-derived nitric oxide to exercise-induced vasodilation. Circulation, *90:* 2853–2858, 1994.
32. Clementi, E., Brown, G. C., Foxwell, N., and Moncada, S. On the mechanism by which vascular endothelial cells regulate their oxygen consumption. Proc. Natl. Acad. Sci. USA, *96:* 1559–1562, 1999.
33. Duplain, H., Burcelin, R., Sartori, C., Cook, S., Egli, M., Lepori, M., Vollenweider, P., Pedrazzini, T., Nicod, P., Thorens, B., and Scherrer, U. Insulin resistance, hyperlipidemia, and hypertension in mice lacking endothelial nitric oxide synthase. Circulation, *104:* 342–345, 2001.
34. Pavlovic, M., Wroblewski, K., Manevich, Y., Kim, S., and Biaglow, J. E. The importance of choice of anaesthetics in studying radiation effects in the 9L rat glioma. Br. J. Cancer, *27:* S222–S225, 1996.
35. Ferrannini, E., and Mari, A. How to measure insulin sensitivity. J. Hypertens., *16:* 895–906, 1998.
36. Ferrannini, E., Haffner, S. M., and Stern, M. P. Essential hypertension: an insulin-resistant state. J. Cardiovasc. Pharmacol., *15:* S18–S25, 1990.
37. Johnson, R. T., Collins, A. R., Squires, S., Mullinger, A. M., Elliott, G. C., Downes, C. S., and Rasko, I. DNA repair under stress. J. Cell Sci. Suppl. *6:* 263–288, 1987.
38. Jayanth, V. R., Belfi, C. A., Swick, A. R., and Varnes, M. E. Insulin and insulin-like growth factor-1 (IGF-1) inhibit repair of potentially lethal radiation damage and chromosome aberrations and alter DNA repair kinetics in plateau-phase A549 cells. Radiat. Res., *143:* 165–174, 1995.
39. Griffin, R. J., Makepeace, C. M., Hur, W. J., and Song, C. W. Radiosensitization of hypoxic tumor cells *in vitro* by nitric oxide. Int. J. Radiat. Oncol. Biol. Phys. *36:* 377–383, 1996.
40. Mitchell, J. B., Wink, D. A., DeGraff, W., Gamson, J., Keefer, L. K., and Krishna, M. C. Hypoxic mammalian cell radiosensitization by nitric oxide. Cancer Res., *53:* 5845–5848, 1993.
41. Biaglow, J. E., Manevich, Y., Leeper, D., Chance, B., Dewhirst, M. W., Jenkins, W. T., Tuttle, S. W., Wroblewski, K., Glickson, J. D., Stevens, C., and Evans, S. M. MIBG inhibits respiration: potential for radio- and hyperthermic sensitization. Int. J. Radiat. Oncol. Biol. Phys., *42:* 871–876, 1998.
42. Snyder, S. A., Lanzen, J. L., Braun, R. D., Rosner, G., Secomb, T. W., Biaglow, J., Brizel, D. M., and Dewhirst, M. W. Simultaneous administration of glucose and hyperoxic gas achieves greater improvement in tumor oxygenation than hyperoxic gas alone. Int. J. Radiat. Oncol. Biol. Phys., *51:* 494–506, 2001.
43. Herold, D. M., Hanlon, A. L., and Hanks, G. E. Diabetes mellitus: a predictor for late radiation morbidity. Int. J. Radiat. Oncol. Biol. Phys., *43:* 475–479, 1999.
44. Kozubik, A., and Pospisil, M. Adaptation to intermittent fasting as a factor modifying the radiation resistance of mice. Experientia (Basel), *38:* 958–959, 1982.
45. Kozubik, A., and Pospisil, M. Protective effect of intermittent fasting on the mortality of γ-irradiated mice. Strahlentherapie, *158:* 734–738, 1982.
46. Lindholm, P., Leskinen-Kallio, S., Kirvela, O., Nagren, K., Lehikoinen, P., Pulkki, K., Peltola, O., Ruotsalainen, U., Teras, M., and Joensuu, H. Head and neck cancer: effect of food ingestion on uptake of C-11 methionine. Radiology, *190:* 863–867, 1994.